PROCEEDINGS OF SPIE

SPIEDigitalLibrary.org/conference-proceedings-of-spie

Simulation of the effect of purulent content of the maxillary sinuses on the transillumination signal

Bryanskaya, E., Gneushev, R. Yu., Novikova, I., Dremin, V., Dunaev, A.

E. O. Bryanskaya, R. Yu. Gneushev, I. N. Novikova, V. V. Dremin, A. V. Dunaev, "Simulation of the effect of purulent content of the maxillary sinuses on the transillumination signal," Proc. SPIE 11845, Saratov Fall Meeting 2020: Optical and Nanotechnologies for Biology and Medicine, 118450U (4 May 2021); doi: 10.1117/12.2591004

SPIE.

Event: Saratov Fall Meeting 2020, 2020, Saratov, Russian Federation

Simulation of the effect of purulent content of the maxillary sinuses on the transillumination signal

E.O. Bryanskaya[a], R.Yu. Gneushev[a], I.N. Novikova[a], V.V. Dremin[a,b], A.V. Dunaev[a]
[a]R&D Center of Biomedical Photonics, Orel State University, Orel 302026, Russia
[b]College of Engineering and Physical Sciences, Aston University, Birmingham B4 7ET, UK

ABSTRACT

In this paper the optical properties of the purulent content of the maxillary sinuses were obtained by spectrophotometry. Based on the obtained absorption and reduced scattering coefficients, a numerical simulation by Monte Carlo method was performed to determine the pattern of light scattering passing through the maxillary sinus with purulent contents. The results of the simulation showed that in transillumination methods for the detection of purulent pathological changes, it is more informative to use the radiation sources with 980 nm.

Keywords: optical diagnostics, diaphanoscopy, spectrophotometry, maxillary sinuses, inflammatory diseases, purulent sinusitis, optical properties, Monte Carlo simulation.

1. INTRODUCTION

Nowadays, optical diagnostic methods are increasingly used in medicine due to their portability, cost-effectiveness and non-invasiveness. Although the use of optical radiation in comparison with x-ray radiation is tools to determine tissue structure only conditionally, at the same time, optical methods based on tissue transmission in the visible and infrared spectral ranges do not have a radiation exposure, which makes it possible to reconduct studies, as well as conduct rapid screening diagnostics.

One of these methods is digital diaphanoscopy (or transillumination) of the maxillary sinuses[1–4]. This method has a long history of usage[4,5], especially in ophthalmology[6] and urology[7]. The previously conducted studies of pathological changes in the maxillary sinuses by digital diaphanoscopy[1,2] have shown that the diagnostic results are determined primarily by the optical properties of the studied area and their changes in various anatomical and gender characteristics of patients, as well as by the presence of various pathologies (cyst, tumor tissue). To clarify the magnitude of signal attenuation during its passage through the sinus with pathology, a numerical simulation by the Monte Carlo (MC) method was previously performed. Note, as optical characteristics of the cystic fluid of the maxillary sinuses, the characteristics of the cystic fluid of the breast tissues were used, while modeling for the case of purulent sinusitis was not carried out[2,8].

The aim of this work was to refine the optical characteristics of a pathological changes (purulent sinusitis) by spectrophotometry and numerical simulation of the study area, taking into account the registered optical characteristics.

2. MATERIAL AND METHODS

Numerical simulation by the MC method is associated with the identification of the optical characteristics of biological tissues used in the model, in particular, the absorption and scattering coefficients. To achieve the work aim, namely, to determine the optical characteristics of the purulent contents of the maxillary sinuses, measurements were made using the Shimadzu UV 2600 spectrophotometer (Japan) with an integral sphere module for wavelengths of 400-1200 nm with a step of 1 nm. The absorption and reduced scattering coefficients were calculated by the “addition-doubling” method.

The refined numerical simulation was performed by the MC method in the TracePro software environment (Lambda Software) using the obtained coefficients for the case of the presence of pus in the sinus. This method is one of the most effective simulation tools when dealing with biological tissues[9,10]. At the same time, the size of the sinuses and the thickness of the biological layers were averaged within the same sex and age, since these values can vary greatly depending on these two factors[11–17]. Additionally, the optical characteristics corresponded to the characteristics selected in the previous simulation[2,8].

*bryanskayae@mail.ru; phone 7 4862 419837; bmecenter.ru/en

Saratov Fall Meeting 2020: Optical and Nano-Technologies for Biology and Medicine, edited by
Valery V. Tuchin, Elina A. Genina, Proc. of SPIE Vol. 11845, 118450U · © 2021 SPIE
CCC code: 1605-7422/21/$21 · doi: 10.1117/12.2591004

3. EXPERIMENTAL RESULTS AND DISCUSSION

The spectra of the obtained coefficients of purulent contents are shown in Figure 1. The optical characteristics of the purulent contents at the wavelengths of the probe applicator LEDs are presented in Table 1.

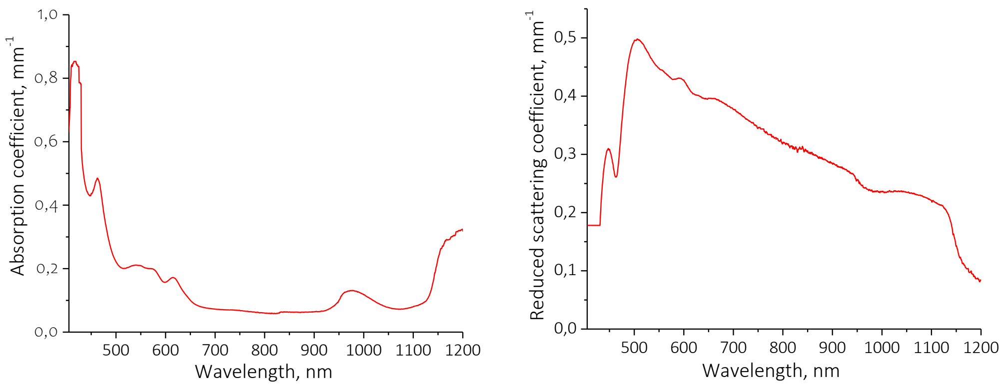

a) b)

Figure 1. The absorption coefficient (a) and the reduced scattering coefficient (b) of purulent contents.

Table 1. Optical characteristics of purulent contents

Layer of biological tissue	Wavelength λ, nm	Absorption coefficient μ_a, mm^{-1}	Reduced scattering coefficient μ'_s, mm^{-1}
Purulent contents	650	0,1005	0,3964
	850	0,06353	0,3062

Based on these measurements, numerical modeling was performed for two radiation sources of the experimental setup[2] with wavelengths of 650 nm and 850 nm (power of 8 mW). The number of simulated photons was 10^6.

Figures 2-3 show the simulation results of the probe radiation propagation (the photons path through the biological tissue and the irradiance map) for the maxillary sinus of female (a) and male (b) without pathology (Figure 2), and with pus (Figure 3).

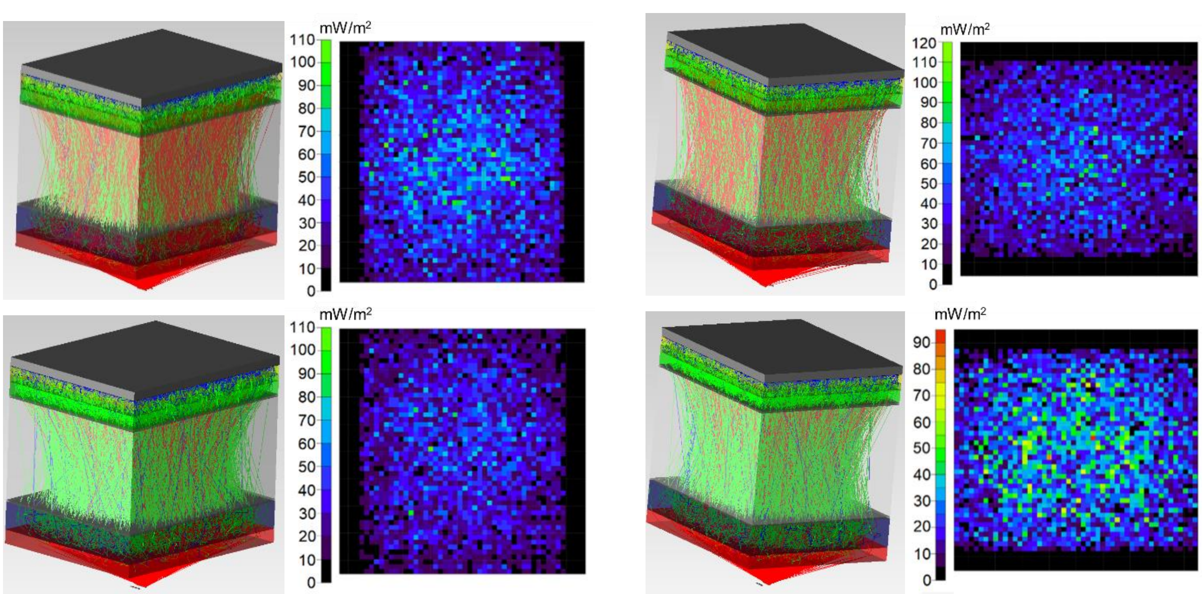

a) b)

Figure 2. Simulation results for the probe radiation propagation through the maxillary sinus of female (a) and male (b) without pathology at a wavelength of 650 nm (top) and 850 nm (bottom).

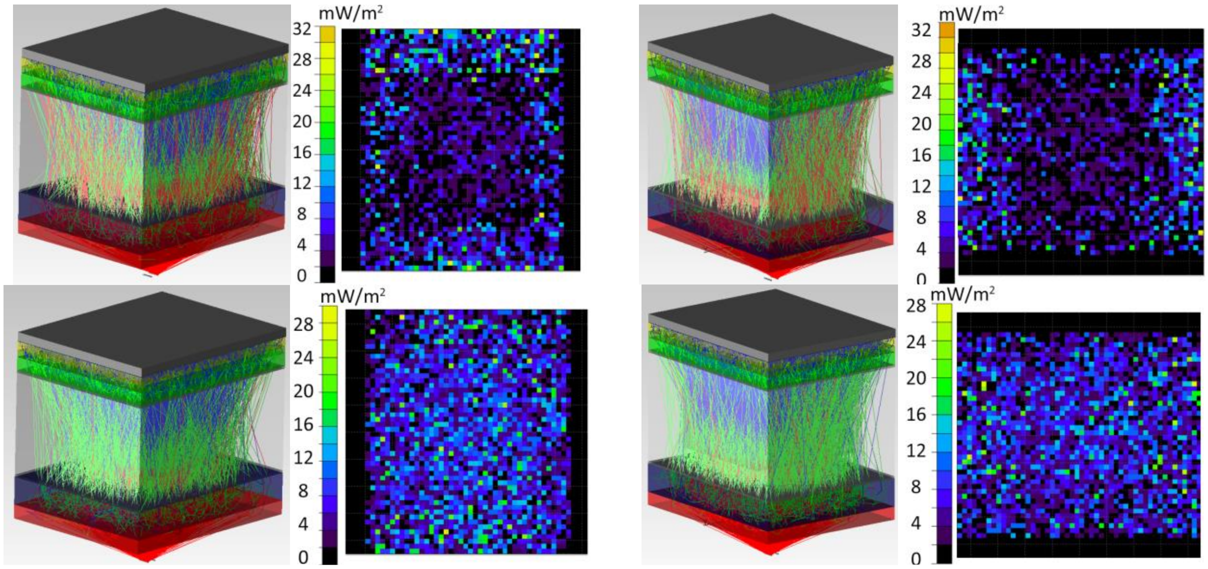

a) b)

Figure 3. Simulation results for the probe radiation propagation through the maxillary sinus of female (a) and male (b) with pus at a wavelength of 650 nm (top) and 850 nm (bottom).

The obtained results showed a decrease in the intensity of optical radiation when passing through the sinus with purulent contents (Figure 4). This decrease has a more pronounced character when the pathology in the sinuses is observed in wavelength 650 nm and can be attributed to the optical features of pathological tissues, namely, the high absorption properties at selected wavelength.

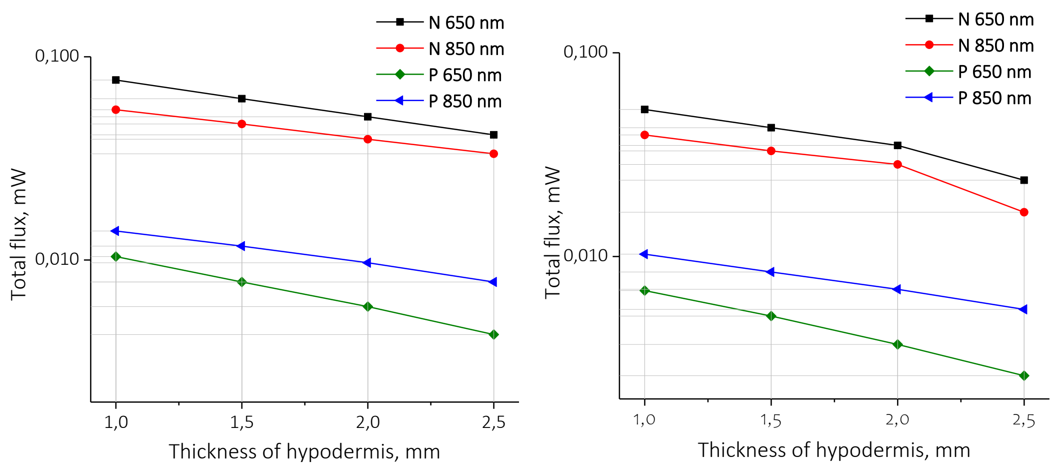

a) b)

Figure 4. Dependence of the change in the total flux (power) of radiation coming to the camera detector on the change in the hypodermis thickness and on the presence of pathology in the sinuses of female (a) and males (b) for wavelengths of 650 and 850 nm. The following labels are used: “N” for healthy tissues, and, “P” for tissues with pus.

An additional analysis of the obtained scattering and absorption spectra of pus presented in Figure 1 showed that for the detection of these pathological changes, it is more informative to use the radiation sources with 980 nm. The absorption μ_a and reduced scattering μ'_s coefficients of light at that wavelength were equal to 0.1303 mm^{-1} and 0.2383 mm^{-1}, accordingly. Based on this, a numerical simulation of the propagation of optical radiation through the sinus with purulent contents for this wavelength was performed (Figure 5).

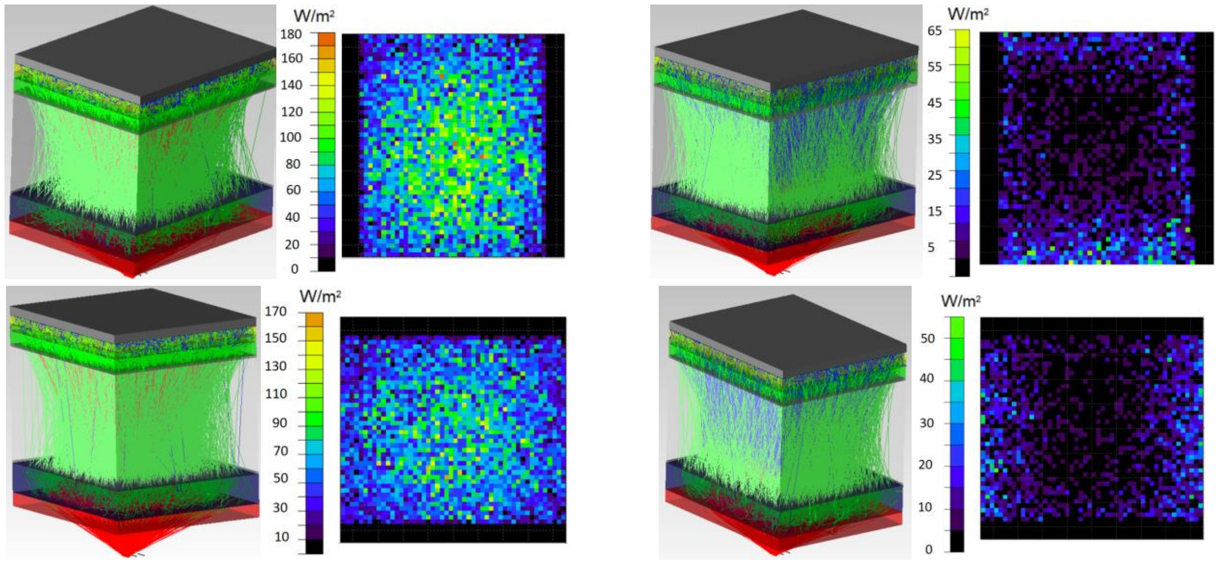

Figure 5. Simulation results for the probe radiation propagation through the maxillary sinus of female (top) and male (bottom) without pathology (a) and with pus at a wavelength of 980 nm.

The analysis of the simulation showed a decrease in the intensity of optical radiation both in male and in female when using a source with a wavelength of 980 nm for probing the sinus with pathology (Figure 6). These results are confirmed by the data obtained with the spectrophotometer.

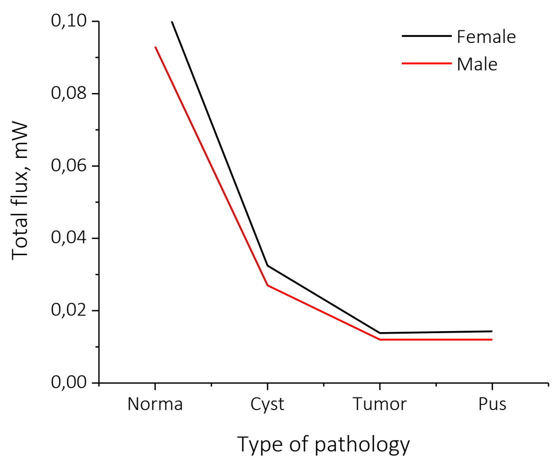

Figure 6. Dependence of the changes in the total flux (power) of radiation coming to the camera detector on the presence of pathology in the sinuses of female and males for wavelengths of 980 nm.

The revealed feature will be considered when adjusting the parameters of the probing and measuring parts of the device that implements the digital diaphanoscopy technology.

4. CONCLUSION

Taking into account the obtained results, the probing part of digital diaphanoscope will be adjusted, namely, in addition to the existing radiation sources, LEDs with a wavelength of 980 nm will be added. This will make it possible to carry out a methodological substantiation of the instrument and algorithmic implementation of this technology, considering various pathological changes, including purulent contents.

ACKNOWLEDGMENT

The reported study was funded by RFBR according to the research project № 20-32-90147. The work was also supported by the grant of the President of the Russian Federation for state support of young Russian scientists № MK-2634.2019.8. V.D. kindly acknowledges personal support from the European Union's Horizon 2020 research and innovation programme under the Marie Skłodowska-Curie grant agreement No. 839888.

REFERENCES

[1] Bryanskaya, E. O., Makovik, I. N., Bukin, A. G., Bibikova, O. A., Shuraev, B. M., Minet, O., Zabarylo, U., Dunaev, A. V. and Artyushenko, V. G., "Diagnosis of inflammatory diseases of the paranasal sinuses using digital diaphanoscopy," Proc. SPIE, 11073P (2019).

[2] Bryanskaya, E. O., Novikova, I. N., Dremin, V. V, Gneushev, R. Y., Bibikova, O. A., Dunaev, A. V and Artyushenko, V. G., "Optical Diagnostics of the Maxillary Sinuses by Digital Diaphanoscopy Technology," Diagnostics **11**(1), 77 (2021).

[3] Stölzel, K., Szczepek, A. J., Olze, H., Koß, S., Minet, O. and Zabarylo, U., "Digital diaphanoscopy of the maxillary sinuses: A revival of optical diagnosis for rhinosinusitis," Am. J. Otolaryngol. - Head Neck Med. Surg. **41**(3), 102444 (2020).

[4] Beuthan, J., "IR-diaphanoscopy in medicine," Med. Opt. Tomogr. Funct. Imaging Monit. **10311**, 263–282 (1993).

[5] Feldmann, H., "Die Geschichte der Diaphanoskopie," Laryngo-Rhino-Otologie **77**(05), 297–304 (1998).

[6] Koch, F. H. J., Deuchler, S., Singh, P. and Heßling, M., "Diaphanoskopie am Auge," Der Ophthalmol. **114**(9), 857–864 (2017).

[7] Schips, L., Lipsky, K., Hebel, P., Hutterer, G., Gidaro, S., Petritsch, P. H. and Zigeuner, R. E., "Laparoscopic fenestration of lymphoceles after kidney transplantation with diaphanoscopic guidance," Urology **66**(1), 185–187 (2005).

[8] Bryanskaya, E. O., Gneushev, R. Y., Makovik, I. N., Dremin, V. V., Bukin, A. G., Bibikova, O. A., Shuraev, B. M., Minet, O., Zabarilo, U., Dunaev, A. V. and Artyushenko, V. G., "Monte Carlo simulation of signals in digital diaphanoscopy of the maxillary sinuses," Proc. SPIE, 11457P (2020).

[9] Dremin, V., Zherebtsov, E., Bykov, A., Popov, A., Doronin, A. and Meglinski, I., "Influence of blood pulsation on diagnostic volume in pulse oximetry and photoplethysmography measurements," Appl. Opt. **58**(34), 9398–9405 (2019).

[10] Zherebtsov, E., Dremin, V., Popov, A., Doronin, A., Kurakina, D., Kirillin, M., Meglinski, I. and Bykov, A., "Hyperspectral imaging of human skin aided by artificial neural networks," Biomed. Opt. Express **10**(7), 3545–3559 (2019).

[11] Kang, S., Lee, S. J., Ahn, S. J., Heo, M. S. and Kim, T. W., "Bone thickness of the palate for orthodontic mini-implant anchorage in adults," Am. J. Orthod. Dentofac. Orthop. **131**(4), 74–81 (2007).

[12] Wara-aswapati, N., Pitiphat, W., Chandrapho, N., Rattanayatikul, C. and Karimbux, N., "Thickness of Palatal Masticatory Mucosa Associated With Age," J. Periodontol. **72**(10), 1407–1412 (2001).

[13] Gracco, A., Lombardo, L., Cozzani, M. and Siciliani, G., "Quantitative evaluation with CBCT of palatal bone thickness in growing patients," Prog. Orthod. **7**(2), 164–174 (2006).

[14] Barghouth, G., Prior, J. O., Lepori, D., Devoisin, B., Schnyder, P. and Gudinchet, F., "Paranasal sinuses in children: Size evaluation of maxillary, sphenoid, and frontal sinuses by magnetic resonance imaging and proposal of volume index percentile curves," Eur. Radiol. **12**(6), 1451–1458 (2002).

[15] Uchida, Y., Goto, M., Katsuki, T. and Akiyoshi, T., "Measurement of the maxilla and zygoma as an aid in installing zygomatic implants," J. Oral Maxillofac. Surg. **59**(10), 1193–1198 (2001).

[16] De Greef, S., Claes, P., Vandermeulen, D., Mollemans, W., Suetens, P. and Willems, G., "Large-scale in-vivo Caucasian facial soft tissue thickness database for craniofacial reconstruction," Forensic Sci. Int. **159**(1), 126–146 (2006).

[17] Xu, X., Zhao, S., Liu, H., Sun, Z., Wang, J. and Zhang, W., "An Anatomical Study of Maxillary-Zygomatic Complex Using Three-Dimensional Computerized Tomography-Based Zygomatic Implantation," Biomed Res. Int. **2017**, 8027307 (2017).